13 Network Organisation of Mycelial Fungi

M. Fricker[1], L. Boddy[2], D. Bebber[1]

CONTENTS

I. Introduction

Filamentous fungi grow out from a spore or an inoculum, by apical extension of slender hyphae that then branch sub-apically to form a fractal, tree-like mycelium. In ascomycetes and basidiomycetes, tangential hyphal fusions or anastomoses occur as the colony develops to form an interconnected mycelial network (Rayner et al. 1994, 1999; Glass et al. 2000, 2004). The basic sequence of morphological events leading to fusion has been well described, most notably by Buller (1931, 1933; summarised by Gregory 1984), and details of the underlying cellular and molecular events are beginning to be elucidated in model systems such as *Neurospora* and *Colletotrichum* (Glass et al. 2000, 2004; Hickey et al. 2002; Roca et al. 2003,

2004, 2005a, b; Fleissner et al. 2005). In the larger, more persistant saprotrophic and ectomycorrhizal basidiomycetes, the network architecture develops further as the colony grows with the formation of specialised high-conductivity channels, termed cords, through aggregation and limited differentiation of hyphae (Cairney 2005). Cords tend to be well insulated from the environment and are able to translocate nutrients between separate food resources or to and from the foraging margin (Boddy 1999; Leake et al. 2004). At the same time as cords form, the intervening regions of the mycelium regress and are presumably recycled to support new growth. The resulting structure and scale of the corded network vary between species, and give rise to qualitatively different, recognisable network architecture (Fig. 13.1). These networks are not static, but are continuously reconfigured in response to local nutritional or environmental cues, damage or predation, through a combination of new growth, branching, fusion or regression (Boddy 1999; Leake et al. 2004). Furthermore, a single genetically identical individual network (genetic mycelial unit, or GMU *sensu* Olsson 2001) can undergo quantum shifts in size through fragmentation, leading to several separate functional mycelial units (FMU; Olsson 1999, 2001). Conversely, fusion of separate FMUs in the following growth season can rapidly (re-)generate a more expansive network (Rayner et al. 1994; Boddy 1999; Leake et al. 2004).

Whilst the largest mycelial networks that are typically grown in laboratory microcosms range over 0.1–1.0 m^2, in an undisturbed forest ecosystem almost all trees and fallen plant parts are interconnected by a diverse population of mycelial systems forming an extensive network over a much larger physical scale termed the 'wood wide web' (WWW; Read 1997; Simard et al. 1997; Simard and Durall 2004). There is considerable evidence for extensive nutrient uptake and exchange through the WWW (Simard et al. 1997; Read and Perez-Moreno 2003; Leake et al. 2004; Simard and Durall 2004).

[1] Department of Plant Sciences, University of Oxford, South Parks Road, Oxford, OX1 3RB, UK
[2] Cardiff School of Biosciences, Cardiff University, Cardiff, CF10 3US, UK
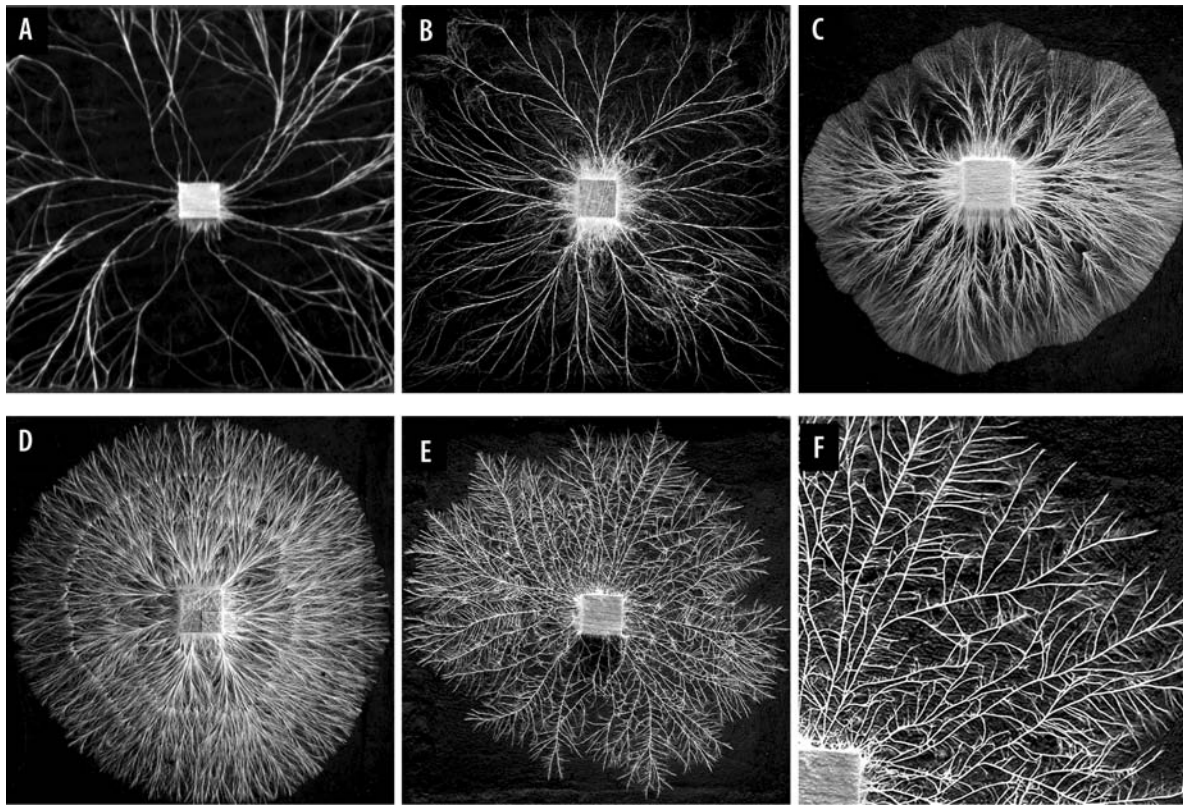
Fig. 13.1. Colony morphology and network architecture for different species of saprotrophic basidiomycetes. **A–F** Mycelial systems of *Resinicium bicolor* (**A**), *Phanerochaete velutina* (**B**), *Hypholoma fasciculare* (**C**), *Coprinus picaceous* (**D**) and *Phallus impudicus* (**E, F**) growing from wood blocks of 2 cm side in 24×24 cm trays of compressed non-sterile soil to illustrate the range of network architecture shown by different species. Photos courtesy of G. Tordoff

Fungi, like any other organisms, must partition limited resources among competing requirements. For example, a very dense, highly connected network might have high transport capacity and resilience to damage or attack because of multiple transport pathways. However, it would incur a large material cost of construction per unit area of explored space and would cover new ground slowly. Conversely, a sparse system could extend further for the same material cost, but would risk missing resources and have fewer alternate routes to survive damage and disconnection (Boddy 1993, 1999; Rayner et al. 1994, 1999). We do not know what factors have been most significant in shaping each strategy in evolutionary terms (Pringle and Taylor 2002) or how organisation and integration of such networks can emerge without centralised control (Rayner 1991; Rayner et al. 1994, 1999). However, as a starting point we might envisage that the resulting networks represent an effective balance between cost, exploration, exploitation, transport

efficiency and resilience to damage. Subtle shifts in the developmental process for different species may have effectively weighted the relative importance of each these aspects to adapt to different spatial and temporal patterns of resource availability and environmental conditions, giving rise to a set of foraging strategies for each species (Boddy 1999). However, there has been relatively little explicit analysis of the structure of the networks formed, their dynamic behaviour and how both impact on these proposed functions.

In this chapter we explore this relatively uncharted middle ground between the microscopic cellular level dominated by discrete tubular hyphae (reviewed in this series by Trinci et al. 1994) and the macroscopic level of intact colonies (reviewed in this series by Olsson 2001), to see the extent that it is possible to characterise the network aspect of mycelial growth. A few years ago this would have been a daunting task as there was no coherent conceptual framework to describe, meas-

ure, summarise and compare such complex networks. In the 1990s, fractal measures were introduced as useful tools to capture aspects of the network structure as a metric (Ritz and Crawford 1990; Crawford et al. 1993; Donnelly et al. 1995; Mihail et al. 1995; Boddy et al. 1999; Crawford et al. 1999; Boddy and Donnelly 2006). However, a single summary value can only express a small fraction of the complexity in the system, even with sub-sampling of different regions. Recently, considerable advances have been made in network analysis, using concepts and tools emerging from graph theory and statistical mechanics (Strogatz 2001; Albert and Barabasi 2002; Dorogovtsev and Mendes 2002; Newman 2003; Amaral and Ottino 2004). These techniques have been applied to a swathe of complex systems, including biological networks such as protein–protein interactions or food webs, and may provide a useful conceptual framework for quantitative analysis of fungal mycelia. We therefore provide an introduction to some of the theory and terminology used to analyse networks, translated as far as we are able into mycological language. We then evaluate its application to analyse the dynamics, efficiency, resilience and adaptation of self-organised fungal networks at different spatial scales. We also try to set network analysis in context with other approaches to measure and model fungal behaviour, with the expectation that a combination of approaches will be required to understand fungal growth over the enormous range of length scales needed.

II. Conceptual Frameworks for Network Analysis

To use network analysis tools to analyse fungal mycelia, it is necessary to translate the morphological structures observed into an appropriate network representation (Bebber et al., submitted). Our starting assumption is that the fungal mycelium can be represented as a graph by classifying junctions (branch-points and anastomoses) as nodes and the hyphae or cords between nodes as links. It is possible to (manually) extract the network from images of mycelial systems taken at appropriate resolution. We illustrate the process and results using the classic microscopic image of *Coprinus sterquilinus* from Buller (1931; Fig. 13.2A) and images of *Phanerochaete velutina* from our own work (Fig. 13.2C). We have developed a simple software interface to

simplify extraction of the network that is available on request.

At the moment nodes have to be manually chosen as automated segmentation algorithms that are not yet sufficiently robust to extract the network unsupervised. Each node is given a unique identifier and stored as a list together with its Cartesian (x, y) co-ordinates. Links are stored interchangeably either as an adjacency matrix or in a list format that can be imported into a wide range of freely available software packages, such as Pajek (http://vlado.fmf.uni-lj.si/pub/networks/pajek/). As links vary in length (l) and cross-sectional area (a), the links are weighted, i.e. they differ in their connection strength. The diameter and hence area of each cord can be determined using image analysis tools. The material construction cost of each link can be estimated from the volume ($l \times a$), i.e. longer, thicker hyphae or cords are more costly to produce in terms of the mass of material required to build them. Similarly, the predicted transport flux through the network is expected to increase with increasing cross-sectional area, but decrease with link length. The precise relationship between flow and area is less clear. For the extreme case of laminar flow through individual hyphal tubes, flow can scale with r^4 in accordance with the Hagen–Poiseuille equation:

$$\text{Volume flow rate per hub} = \frac{\pi r^4}{8\eta}\frac{\partial P}{\partial x} \qquad (13.1)$$

where r is the radius of the tube, η is the viscosity of the fluid, and $-\delta P/\delta x$ is the negative gradient of the hydrostatic pressure. In multi-hyphal aggregates such as cords, the structure is more akin to a cylinder packed with individual hyphae in parallel. In this case, flow can scale with the area, i.e. r^2, although it is recognised that the internal structure of cords can be more complex, with both larger vessel hyphae increasing potential flow and fibre hyphae that do not contribute to transport.

A. Experimental Analysis of Mycelia as Networks

The *C. sterquilinus* colony (Fig. 13.2A) captures the essence of fungal network formation on a microscopic scale. A sparse branching tree-like structure forms in the peripheral growth zone from tip growth and sub-apical branching, whilst secondary growth and fusion of hyphae in the centre of the colony forms an interconnected network with
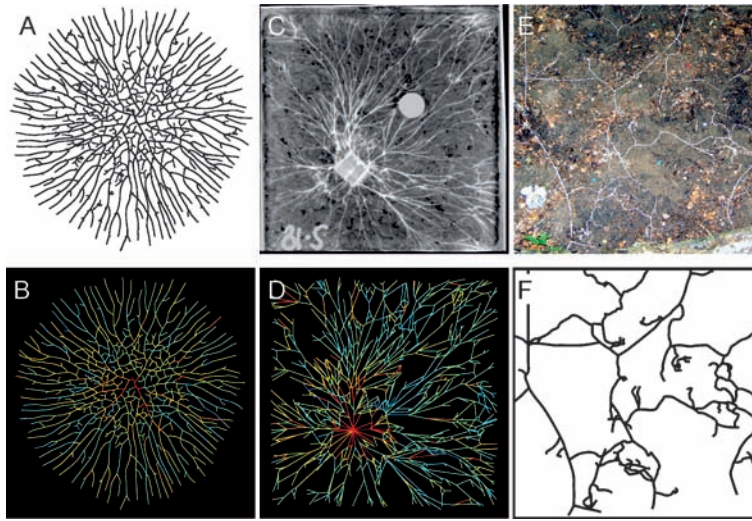
Fig. 13.2. Analysis of mycelial network structures over different length scales. **A** Drawing of a young colony of *Coprinus sterquilinus* showing the development of an anastomosing network in the colony interior. The colony is around 380 µm in diameter (modified from Buller 1931). **B** Network representation of the same colony in which the link weight is colour coded on a rainbow scale, with red representing the thickest hyphae. **C** Mycelial system of *P. velutina* grown from 4 cm³ beech wood inocula on a 24×24 cm tray of non-sterile soil with an inert bait (*grey circle*) after 39 days. Digital images were obtained from photographs taken by R. Bolton. **D** Network representation of the same colony in which the link weight is colour coded on a rainbow scale with red representing the thickest cord. **E** A 75×75 cm portion of an extensive network of the saprotrophic fungus *Megacollybia platyphylla* growing from a log in Wytham Wood, Oxfordshire, UK. **F** A schematic representation of the *P. impudicus* network
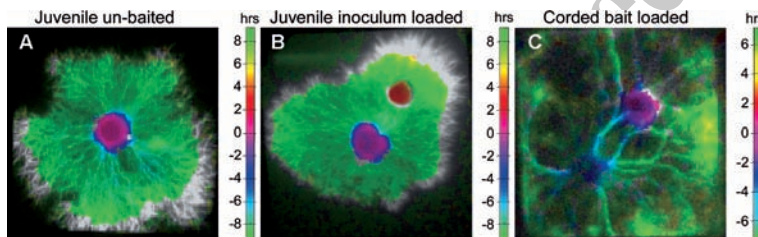

Fig. 13.3. Establishment of oscillatory phase domains in colonies of *P. velutina*. Pseudo-colour-coded images showing the relative phase of the oscillatory component of labelled aminoisobutyrate (^{14}C-AIB) transport determined pixel-by-pixel using Fourier analysis. The colour represents the phase difference in hours (*hrs*) according to the adjacent scale for each image from the oscillation recorded at the loading site. Only regions with the same frequency are colour-coded. Regions with a different frequency or where the Fourier analysis was not possible, such as the growing colony margin, are coded in grey-scale. The period of the oscillation ranged from 18.3 h (**A**, **B**) to 14.2 h (**C**), depending on the growth temperature with a Q_{10} of around 2. **A** Control colony grown for 240 h, showing distinct phase domains in the inoculum and foraging mycelium with ∼7 h phase difference. **B** Development of an additional phase domain in the bait of a juvenile colony. The bait lags the inoculum by ∼3.5 h. **C** Phase map of a 35-day-old colony following loading at the bait, showing distinct phase domains in the bait, inoculum, connecting cords and foraging mycelium

many cycles (Fig. 13.2A). The extracted network representation contains 579 nodes and 656 links (Table 13.1), each with an associated measure of its length and diameter that can be combined to give an estimate of the volume (cost) or predicted resistance to flow (Fig. 13.2B). In theory, larger networks than this can be captured using large-scale mycelial mapping (LSMM; Crawford et al. 1993; Ritz et al. 1996) and analysed at the level of an individual hypha. However, it becomes increasingly difficult to distinguish fusions from overlapping hyphae as the colonies become denser; and the sheer number of

Table. 13.1. A summary of common network measures and their application to fungal mycelia

Topology Measure	Symbol	Description	Example networks Coprinus sterquilinus	Phanerochaete velutina
Nodes (vertices)	N	The total number of connected entities. In the mycelium, these are the branch points, fusions, or tips.	579	986
Links (edges)	M	The total number of connections. In the mycelium, the number of cords or hyphae that connect the vertices. Links can be directed, i.e. flow occurs only in one direction.	656	1351
Node degree	k	The number of links attached to a node. Often used as a measure of the connectedness of networks, especially the frequency distribution of k. This measure is less useful for mycelia as k is usually either 3 (for junctions) or 1 (for tips). Mean k (excluding the highly-connected wood block) is given on the right. Node strength (see below) is more appropriate for weighted networks.	2.26	2.71
Subgraphs	g	If the network is broken up, the number of disconnected parts. Of interest when considering resilience of the mycelium to attack.	1	1
Cyclomatic number (Haggett and Chorley 1969)	$M - N + g$	The number of closed loops or cycles in the network. This gives an indication of the number of redundant pathways in the mycelium.	78	366
α−index (Haggett and Chorley 1969)	$\alpha = \frac{M-N+g}{2N-5}$	The number of cycles normalised by the possible maximum (assuming no overlapping links), taking values from 0 to 1 to allow comparison of networks of different sizes. This measure has been described as 'meshedness' (Buhl et al. 2004).	0.07	0.19
Clustering coefficient (Watts and Strogatz 1998)	C	A measure of the number of cycles, or loops, of length 3 (i.e. triangles) in the network. Takes values from 0 to 1. Useful for describing the connectedness of some types of network, but less so for fungal networks and many other spatial networks, as their construction often precludes the formation of triads.	0.01	0.11
Spatial structure				
Spatial extent	A	The area covered by the mycelium. Calculated as the area of the convex hull of the node positions in space or by segmentation of the colony outline.	0.11 mm^2	51,050 mm^2
Node density	NA^{-1}	The number of junctions per unit area of space covered by the mycelium. This is a measure of the branching/fusing density. It is likely that this varies through space and time, indicating the responses of mycelial branching to local conditions. Data may be aggregated using spatial interpolation techniques such as Kriging (Isaaks and Srivastava 1989).	5185 mm^{-2}	0.019 mm^{-2}
Link weight	w	A measure relating to the properties of a link, for example its physical length l or cross-sectional area a. Measures can be combined to predict other properties, such as resistance to transport or volume of cords (see below). Estimating link weight is fundamental to other, more complex, calculations of network properties. Mean a is given on the right.	0.000033 mm^2	0.03 mm^2
Node strength (Barthelemy et al. 2005)	$s = \sum_{i=1}^{k} w_i$	A measure of the importance of a node, calculated by summing the link weights w of all the k links connected to a node. For example, the (trimmed) mean value of the node strengths (ignoring the central wood block), calculated as the sum of link cross-sectional areas, is given on the right. This measure is regarded as more informative than node degree for weighted networks.	0.000075 mm^2	0.09 mm^2
Total length	$L = \sum_{i=1}^{L} l_i$	The total length of links in the network, calculated by summing the lengths of all links in the network.	12.2 mm	12,600 mm

Topology Measure	Symbol	Description	Example networks Coprinus sterquilinus	Phanerochaete velutina
Total volume (cost)	$V = \sum_{i=1}^{L} l_i a_i$	An estimate of the material construction cost of the network, calculated summing the estimated volumes (la) of each link. Actual mass can be estimated if the density of cords is known. This could be extended to the mass of carbon, nitrogen, or other components making up the mycelium.	0.00038 mm^3	391 mm^3
Volume density	VA^{-1}	The amount of mycelium per unit area. Gives an estimate of the efficiency of mycelium in covering space.	0.017 $\frac{\text{mm}^3}{\text{mm}^2}$	0.008 $\frac{\text{mm}^3}{\text{mm}^2}$
K-function (Ripley 2004)	$K(t) = nAN^{-1}$	The K-function provides an estimate of the spatial clustering of points, in this case nodes. K for a particular radius t around a node is the average number of nodes within t of that node, divided by the total node density. $K(t)$ can be compared with expected values for a completely random (Poisson) distribution to detect clustering of nodes at different spatial scales.	–	–
Mass fractal dimension	$n(s) \approx cs^{-d}$	Mycelia can be described as fractals over certain length scales, as they fill space more than a line but less than a continuous plane (Boddy and Donnelly 2006). The box counting method overlays a series of grids of square boxes with side length s onto an image of the network. The number of boxes that intersect the image $n(s)$ is related to s via the fractal dimension d.	–	–
Transport Resistance	$r \propto la^{-1}$	Resistance is a measure of the difficulty transporting material through a link, proportional to length divided by cross-sectional area, so that long, thin links have greater resistance. Resistance can be thought of as analogous to expected travel time in road networks, or electrical resistance in electrical networks of resistors. The inverse of resistance is conductance (al^{-1}). Resistance is a fundamental measure in estimating transport through the network. Resistance can be used in electrical resistance network models to provide estimates of flux through the mycelium. Mean resistance for the fungal network is given on the right.	690 $\frac{\text{mm}}{\text{mm}^2}$	585 $\frac{\text{mm}}{\text{mm}^2}$
Shortest path (see Dorogovtsev and Mendes 2002)	$d_{ij} = \sum_{h=1}^{g} r_h$	The shortest path, or geodesic path, between nodes i and j is the path of least resistance. There are g links in the shortest path. There may be more than one path with the smallest sum of resistances, and several paths with sums of resistances very close to the smallest sum. We expect the maximum rate of transport of material along the shortest path. The shortest path is a fundamental measure of network transport. However, it fails to take into account parallel pathways in predicting flux which may be captured better using electrical circuit analogues (see above).	–	–
Diameter (see Dorogovtsev and Mendes 2002)	$D = \max(d_{ij})$	The diameter of the network is the longest shortest path. Although widely used in graph theoretic approaches for unweighted networks, in fungal networks this measure is highly sensitive to the presence of a very long, thin connection, usually a peripheral cord in the case of a mycelial network.	14,818 $\frac{\text{mm}}{\text{mm}^2}$	18,980 $\frac{\text{mm}}{\text{mm}^2}$
Average shortest path	$\ell = \frac{1}{N(N-1)} \sum_{i \neq l} d_{ij}$	The average shortest path provides a measure of the overall transport efficiency of the network. Networks of similar physical extent which have smaller average shortest paths have a more efficient transport system.	5061 $\frac{\text{mm}}{\text{mm}^2}$	5474 $\frac{\text{mm}}{\text{mm}^2}$

Topology Measure	Symbol	Description	Example networks Coprinus sterquilinus	Phanerochaete velutina
Global efficiency (Latora and Marchiori 2001, 2003)	$E_{glob} = \frac{1}{N(N-1)}\sum_{i\neq j}\frac{1}{d_{ij}}$	The *efficiency* measure was introduced (Latora and Marchiori 2001) to overcome a difficulty with the average shortest path, namely that for disconnected networks the shortest path could be infinite (i.e. for two nodes in separated subgraphs). In the efficiency calculation, the mean reciprocal of the shortest path is calculated; and the reciprocal for disconnected nodes is defined as zero.	$0.00028\ \dfrac{\mathrm{mm}^2}{\mathrm{mm}}$	$0.00032\ \dfrac{\mathrm{mm}^2}{\mathrm{mm}}$
Betweenness centrality (Freeman 1977)	$B_u = \sum_{ij}\frac{\sigma_{iuj}}{\sigma_{ij}}$	Betweenness centrality is a measure of the importance of a node or link to transport. The betweenness centrality of a node or link u is the proportion of all shortest paths between pairs of nodes i and j, σ_{ij} that pass through u, σ_{iuj}. Loss of the node or link with the highest betweenness centrality leads to the most increases in shortest path lengths.	–	–
Central point dominance (Freeman 1977)	$CPD = \frac{1}{N-1}\sum_i(B_{max} - B_i)$	Central point dominance (CPD) measures the relative importance of the node with the largest betweenness centrality (B_{max}), compared with all other nodes. For a star-like network CPD = 1, because all shortest paths pass through the central node and only one shortest path through all other nodes.	0.50	0.62
Resilience Relative diameter	$D_{rel} = D^*/D$	Removal of nodes or links should increase the shortest paths in the network, thereby increasing the diameter (and mean shortest path). Relative diameter is the diameter of a disturbed network D^* scaled by the original diameter D. However, fragmentation of the network into subgraphs leads to infinite shortest paths, making this measure difficult to apply in many circumstances.	–	–
Vulnerability (Gol'dshtein et al. 2004)	$V = \frac{E_{glob}-E_{glob}^*}{E_{glob}}$	When nodes or links are removed from a network, the length of shortest paths and number of disconnected nodes is expected to increase, and therefore the global efficiency decreases. Scaling the efficiency of a disturbed network ( ) by the original efficiency gives a measure of the disturbance. Calculating V for removal of a single node or link gives the vulnerability for that node or link.	–	–
Reachability (availability; Ball and Provan 1983)	$R = \frac{2P}{N(N-1)}$	Reachability is the number of paths between nodes that exist in the network P, divided by the possible number of paths (i.e. $N(N-1)/2$). Fragmentation of the network into subgraphs decreases P. Unlike relative efficiency, the measure is independent of the length of shortest paths.	–	–

nodes and links makes manual extraction of the network prohibitively time-consuming. In the future it may be possible to sub-sample segments of the entire colony if suitable methods are developed to deal with the connectedness of nodes and links at the artificial boundaries that this introduces.

The next appropriate level of resolution in practical terms are microcosms in the centimetre to metre range where the dominant structure is a corded mycelium (Figs. 13.1, 13.2C,D). In the case of the *P. velutina* grown in a 24-cm square microcosm, the size of the corded experimental networks reaches around 500–1500 nodes (Fig. 13.2C; Bebber et al., submitted). It might be appropriate to consider the links to be directed on the basis of their initial growth direction. However, in practice, the physiological direction of nutrient fluxes is more important and does not have to follow the developmental connection sequence. Unfortunately, we cannot predict *a priori* which direction the flux may move in and, indeed, we expect it to vary depending on the source–sink relationships within the network. In the future, the techniques to map fluxes described below (Sect. IV.) may provide this information, but at this stage it is simpler to assume that links are undirected and capable of moving nutrients in either direction. The reader is referred to the chapter by Ashford and Allaway (Chap. 2 in this volume) for a discussion of the possible role of vacuolar transport mechanisms for trans-cellular movement of materials over long distances.

In theory, the same approaches can be used for networks in the field. However, the structure is more difficult to capture from simple photographs (Fig. 13.2E) as the network requires careful excavation and additional on-site notes to define contiguous cords. Thus, at this stage it is relatively easy to extract a schematic representation of the network (Fig. 13.2F), but rather more difficult to perform a robust quantitative analysis.

B. Common Network Measures

Once the weighted network has been digitised, a wide range of network parameters can be calculated. Some of the most common ones are given in Table 13.1. These values either have a straightforward biological meaning in their own right or they provide a comparison with network structures in other domains. As the data are embedded in Euclidean space, a number of basic morphological measures can be readily derived. An insight into

the behaviour of the mycelial network can then be gleaned by following the trajectory for each parameter over time (Bebber et al., submitted). For example, the area covered by the colony can be estimated from the convex hull (effectively the polygon formed by stretching an elastic band around the outermost points), provided the network is not too sparse (Fig. 13.4A). The sum of the link lengths gives the total length of mycelium present (Fig. 13.4B), whilst including the cross-sectional area of the links gives an estimate of the volume of the fungus that, with appropriate calibration, can be related to the wet or dry weight. Early development in *P. velutina* is characterised by initial diffuse growth and branching of individual hyphae, which then resolve into cords as the growing front moves outward (Fig. 13.2C). Thus global network size measures, such as area, number of nodes and number of links, increase through time (Fig. 13.4A, B). However, the local scale network evolution is characterised by selective loss of connections and thinning out of the fine mycelium and weaker cords that gives rise to a decrease in the network density (cost per unit area) with increasing colony area (Fig. 13.4C). Although these measures provide a compact summary of the whole colony, they disguise any local variations in structure. There are a number of spatial averaging techniques, such as Kriging (Isaaks and Srivastava 1989), to interpolate between the very fine information at the level of each node and the overall colony metrics; and this approach may also facilitate comparison between different replicates and treatments.

A number of different quantities are typically measured for a network to understand its properties better. The degree (k) of each node is given by the number of links associated with that node. Thus tips have a degree of 1 as they are only connected to the previous node and branch points typically have a degree of 3, because the growth processes forming the network tend to give a single branch or a single fusion at each point. Initially overlapping cords often subsequently fuse, which generates $k = 4$ nodes. It is unlikely that there will be any loops where a link curls back around on itself to re-join the same node, although multiple parallel links between two nodes are possible. As the fine structure of the mycelium within a food resource, such as an agar inoculum or wood block, cannot be resolved, each of these is represented as a node with many links, resembling a hub in other network systems.

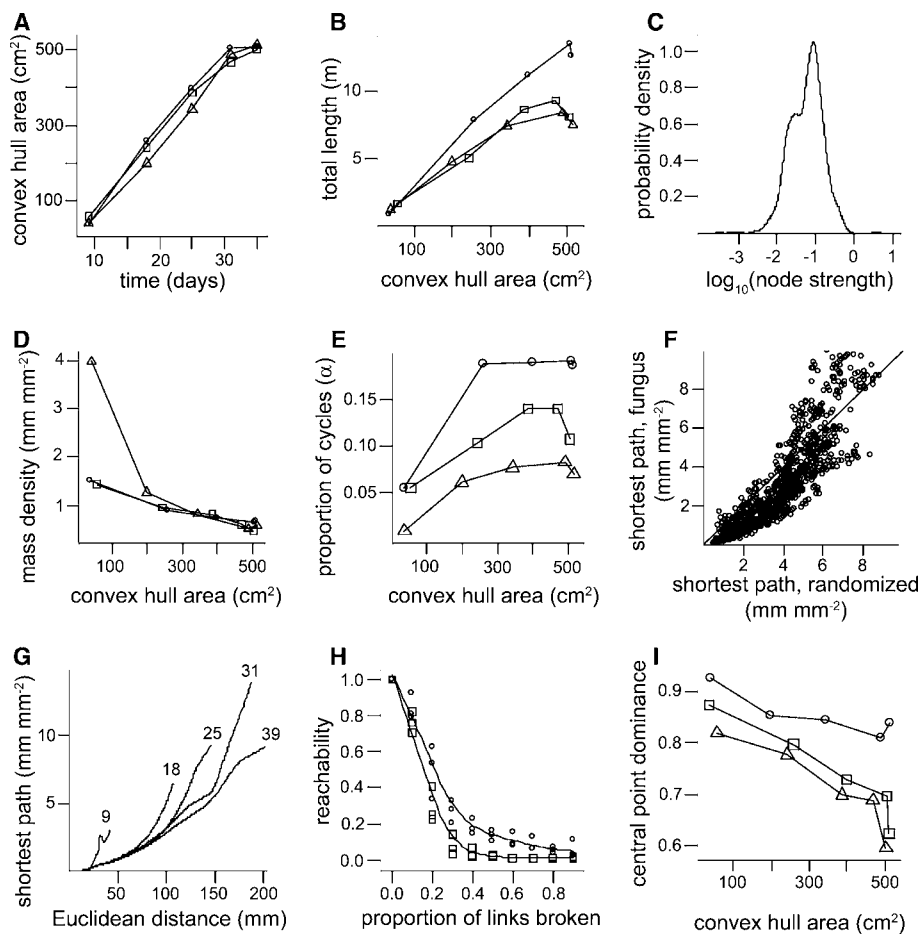Considerable emphasis has been placed on the frequency distribution of node degree in other

Fig. 13.4. Network measures for colonies of *P. velutina*. Mycelial systems of *P. velutina* were grown from 4 cm³ beech wood blocks in 24×24 cm trays of non-sterile soil and photographed at intervals up to 39 days. The weighted network was manually extracted from digitised images and a range of network parameters calculated for three independent time-series. **A** The change in area, measured as the convex hull, with growth of the colonies. **B** The change in mycelium total length as the area increases. **C** The mass density taking into account the varying diameter of the cords. **D** The probability distribution of $\log_{10}$ node strength. **E** The change in the proportion of fundamental cycles (α) with increasing area. **F** Comparison of the shortest path (in 1000s) from the inoculum to every node for the weighted network plotted against the same network with the weights distributed evenly across the links. Points below the diagonal indicate that the fungus is performing better than expected for this null model. **G** Average shortest path distances (in 1000s) plotted against the Euclidean distance from the inoculum for all nodes at the time points indicated. Only means fitted by Friedman's smoother are shown for clarity. Mean values for later stages are smaller than those for earlier stages at a given Euclidean distance, showing that the network increases transport capacity as it develops. **H** The central point dominance (CPD) gives a measure of the decrease in the importance of the inoculum as the network becomes better connected. **I** Change in the reachability of all nodes in the network with progressive removal of links to simulate the effect of grazing. The resilience of the weighted network (*open circles*) is greater than the same network with the weights distributed evenly as a null model (*open squares*)

networks, following the discovery of scale-free distributions in networks from many different domains (Barabasi and Albert 1999). However, the degree distributions for fungal networks are not very informative because of the constraints imposed by the developmental process and crowding effects restricting the maximum number of possible connections, as with other spatial networks (Barrat et al. 2005). In weighted networks, the weighted degree distribution of node strength, measured as the sum of link cross-sectional areas per node, is regarded as a more informative measure to take into account the varying importance of the connections to each node (Barrat et al. 2004).

For the *P. velutina* networks, the frequency distribution of node strength follows an approximately log-normal distribution (Fig. 13.4D).

The next level of organisation up, from a consideration of individual nodes and their summary statistics, is a consideration of the properties of their local neighbourhood. There are several measures that describe how well each node and its neighbours are interconnected. One of the most common is the mean clustering coefficient, C (Watts and Strogatz 1998), defined as the proportion of links connecting a node's immediate neighbours out of the maximum possible number of links. However, C is restricted to the case of cycles with three links forming triads, which is not appropriate to all classes of network, including fungal mycelia, as their construction effectively precludes formation of triads. In practice, the network forms an interconnected reticulate system with many 4-, 5- or 6-node rings spreading away from the central inoculum. Thus more general measures have been proposed to capture the structure of larger cycles (Alon et al. 1997; Caldarelli et al. 2004). The meshedness coefficient was recently introduced to address this point for planar graphs of ant galleries (Buhl et al. 2004; Cardillo et al. 2006). However, the meshedness coefficient is actually a re-discovery of the alpha coefficient originally proposed by the geography community in the 1960s (Haggett and Chorley 1969). Thus we prefer this latter original terminology and measure of closed loops as it has a historical precedent over meshedness (Fig. 13.4E). The shift from essentially a radial tree during early growth to a more reticulate network with increased cross-linking is reflected in an increasing value of the alpha index (Fig. 13.4E). Thus these fungal networks progress from a branching tree to a weakly connected lattice-like network behind the growing margin through a process of fusion and reinforcement to form loops and selective removal and recycling of excess redundant material (Bebber et al., submitted).

C. Predicted Transport Characteristics

To determine the efficiency of nutrient translocation in the mycelial network, the predicted transport performance was assessed. The typical metric used in network analysis is based on the shortest distance between any two nodes and is summarised either as the average, to give the average shortest path through the network, or as the longest shortest path which is termed the diameter of the network. A small average shortest path or a low diameter implies that it is easy to transport material anywhere in the network. However, in weighted mycelial networks, the network diameter is a highly unstable measure of network size as it is extremely sensitive to thin links with very high resistance at the mycelial margin. Thus we have not yet found this a useful network statistic, even for comparison with networks from other domains.

In a spatial graph, the average shortest path and the network diameter is expected to increase as the colony gets bigger, simply because they are defined by the physical distances between the nodes. However, including the predicted consequences of the varying cross-sectional area can significantly alter this view. Thus, thickening of some routes, effectively increasing their transport capacity, reduces the apparent shortest transport path (Bebber et al., submitted). In isolation, it is difficult to attribute meaning directly to this measure. However, one way to assess the significance of the organisation of the weighted links is to compare the actual network with one in which the weights have been either randomised between the links or distributed evenly across all links. Although results from such an analysis can be summarised as the mean shortest path or the diameter, it has proved more informative to consider how the performance changes with radius, not least because this maps onto the developmental sequence of network formation. Thus, over most of the physical radius of the colony, the structure built by the fungus has a lower shortest path than the equivalent structure with the same total material spread evenly across the network (Fig. 13.4F). Near the boundary the two systems become equivalent and right at the margin, where the very fine hyphae are located, the real colony performs much worse than the homogeneous network. As the network grows, previously peripheral nodes, which originally had a long shortest path, become better connected to the inoculum by the development of stronger links (Fig. 13.4G). Thus the branching margin resolves down to a more efficient transport system through thinning out of some links, coupled with reinforcement of retained routes and an increase in their transport capacity (Bebber et al., submitted).

The importance of any node, as a transport hub, can be estimated from the proportion of shortest paths that pass through it, in a measure termed the *betweenness centrality* that was originally used in the social sciences (Freeman 1977). A more specific

measure derived from the betweenness centrality is the *central point dependence* (CPD), which focuses solely on the relative importance of the node with the greatest betweenness centrality. In fungal networks this corresponds typically to the inoculum. Thus the CPD declines from ~90% to ~70% in control networks (Fig. 13.4H) and to ~55% in networks with an additional added wood resource (Bebber et al., submitted). This suggests that the network becomes more decentralised as it grows, forming cross-links that bypass the original inoculum.

Although these network measures provide some indication of the predicted transport efficiency of the mycelial systems, network analysis based on graph theory does not readily capture the importance of many potential parallel pathways for flux through the network, as they are dominated by measures that highlight single (shortest) paths. We have also examined alternative approaches using well developed tools for solving current flow through complex resistor networks (e.g. Hankin 2006). The weighted adjacency matrix from the mycelial network is already in an appropriate form to be recast as an electrical circuit analogue, with the additional constraint that flux (current) through the network can only be calculated if a driving force (voltage) is applied to certain points in the network. This allows what-if type examinations of the expected flux as source–sink patterns change. For example, a map of the predicted current flow from the inoculum to the hyphal tips can be calculated if a voltage is applied at the inoculum and all the tips are grounded.

D. Predicted Network Resilience

Whilst the architecture of the weighted network clearly improved transport efficiency, in nature the same system also has to resist accidental damage or targeted attack by grazers.

In many networks, the probability of node or link removal is unlikely to be random, and may also show a high degree of correlation between adjacent nodes. For example, in the case of fungi, grazing by soil invertebrates may occur at specific locations in the network (Harold et al. 2005). This is because some regions are more palatable or accessible than others. One measure to characterise the vulnerability of the network is to examine the effect of link breakage on global efficiency (E), where E is measured as the sum of the inverse of all shortest paths (Latora and Marchiori 2001). This measure is more

appropriate than just changes in the mean shortest path as it can handle disconnection of parts of the network. In other network analyses it is often the nodes that are attacked. However, for fungal mycelia we believe that discussion of link breakage has more biological relevance. Thus, in a targeted attack, we assume that the probability of link breakage is proportional to length and inversely proportional to area [$P(b) \sim l/a$], i.e. longer, thinner cords are more likely to break. To highlight the importance of the organisation of the weighted links in the network, this can be compared with a model in which the breakage probability is proportional to length alone. The relative global efficiency, E/E_{max}, where E_{max} is the efficiency of the unbroken network, is consistently greater for a given proportion of links broken, when link weighting is taken into account. Thus the distribution of link diameters in the fungal networks significantly increases their resilience to attack. One disadvantage of the vulnerability measure for a weighted network is that consistent removal of the weakest links naturally biases the measure of efficiency, so the decrease in network performance is perhaps not as marked as expected. An alternative measure, termed *reachability* (Ball and Provan 1983), provides an unbiased measure as it only considers the proportion of paths remaining, without reference to their transport capacity (Fig. 13.4H).

Whilst a single metric, such as 50% of the maximum efficiency or number of paths, provides a succinct summary of the resilience of the network, it disguises much of the subtlety in the full response of the fungal systems to attack. Thus the reachability of the weighted network does not decay with a simple function, but is eroded down to a core that is very much harder to destroy than equivalent networks with evenly distributed weights or randomised weights. This suggests that the same core architecture that gives the network good predicted transport properties (see Sect. C.) also gives it good resilience. Interestingly, the predicted pattern following this type of simulated attack closely matches the observed pattern for real mycelial systems of *P. velutina* under attack by particular species of *Collembola* (Fig. 13.5A, B). It is also worth noting that part of the resilience of such a biological network may not be just the architecture of the network prior to damage, but the ease and efficiency with which the network can reconnect itself following attack. In this respect, a self-organising spatial network may have considerable advantages over a random network in the cost, consistency and effi-
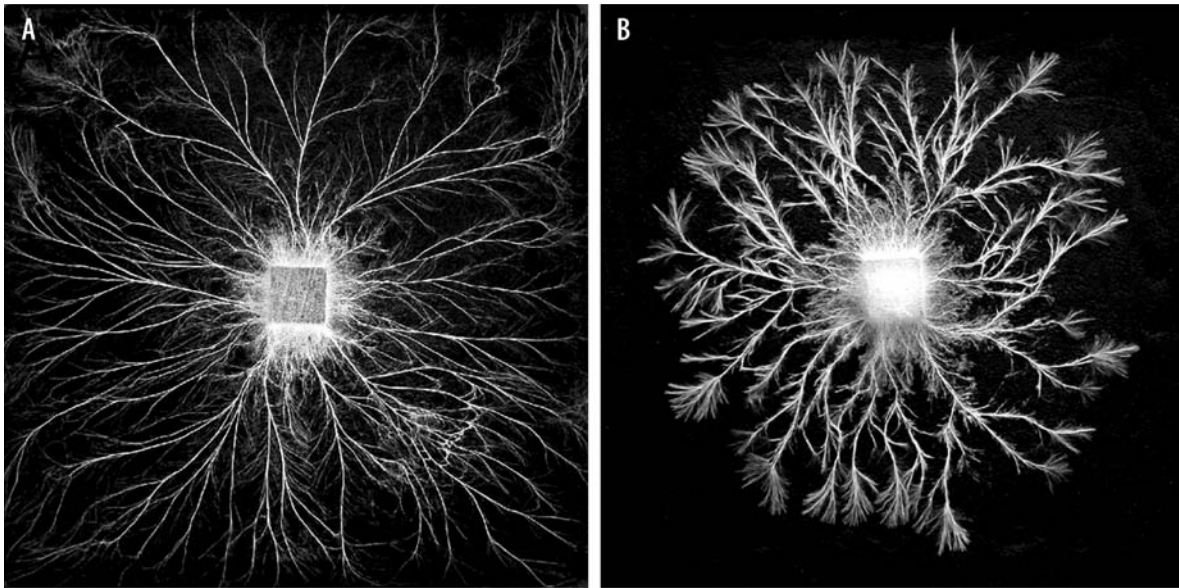
Fig. 13.5. The effect of *Collembola* grazing on networks of *P. velutina*. Mycelial systems of *P. velutina* grown from 4 cm³ beech wood inocula on 24×24 cm trays of non-sterile soil after 21 days in the absence (**A**) and presence (**B**) of *Collembola*. In the presence of grazing, the network is trimmed down to a central core and the frequency of circumferential links increases. In addition there is a profusion of new fine mycelia from the damaged tips. Digital images were obtained from photographs taken by G. Tordoff

cacy of the rewiring process needed to re-establish a functioning system.

III. Comparison with Other Representations of Mycelial Structure and Growth

Network analysis provides a compact description of the fungal mycelium drawn from experimental systems and may provide insights into the underlying developmental processes. However, it is not a mathematical model of the fungal growth process *per se*. In an ideal world it might be possible to infer network construction algorithms from the network structure which would be of use to biologists and may also inform the design and construction of anthropogenic infrastructure networks. Whilst this is still an aspiration, it is instructive to compare the results and expectations of the experimentally derived network representation with other models of colony growth.

A. Continuous Models

There is an extensive literature describing both the cell biology of hyphal tip growth (see the chapters by Bourett et al., Fischer, and Sudbery and Court; respectively Chaps. 1, 5 and 6 in this volume) coupled with increasingly sophisticated mathematical models based around the vesicle supply centre (VSC) model (Bartnicki-Garcia et al. 1989; reviewed by Prosser 1995a, b; Geitmann 2006; see also Sudbery and Court, Chap. 6 in this volume), including extension to three-dimensional models (Gierz and Bartnicki-Garcia 2001; Tindemans et al. 2006). These models provide the raw material for developing models of colony branching patterns, but do not yet include anastomoses. Furthermore, they are probably pitched at too fine a resolution to consider scaling-up to a working model of network formation.

At the level of the colony, a range of different modelling approaches have been applied (Bezzi and Ciliberto 2004). There are several 'continuous models' that seek to model the collective attributes of the mycelium, rather than the growth of individual hyphae, but include morphological features such as tip growth, branching, anastomosis and cell death within the equations (Edelstein 1982; Edelstein and Segel 1983; Edelstein et al. 1983; Edelstein-Keshet and Ermentrout 1989; Davidson et al. 1996, 1997; Davidson and Park 1998; Davidson and Olsson 2000; Boswell et al. 2002, 2003a; Jacobs et al.

2004). In such models growth is driven by nutrient concentration derived from uptake and internal passive or active transport. The most advanced partial differential equation (PDE) model has been developed for *Rhizoctonia solani* and has been calibrated against experimental measurements of key parameters (Davidson et al. 1997; Davidson 1998; Davidson and Olsson 2000; Boswell et al. 2002, 2003a). Predictions from the model match experimental observations for systems growing on tessellated heterogeneous resources (Jacobs et al. 2004), but the equations are difficult to solve mathematically (Boswell et al. 2003b) and effectively limit computation to a simulation of growth over a few centimetres and a few hours. Nevertheless, these models provide good descriptions of mass and substrate distributions for growth in both homogeneous and heterogeneous environments. One of the disadvantages of this basic PDE approach is that it can only describe the architecture of the mycelium through its average properties, such as branches and fusions per unit area, since it does not have an explicit morphological representation of the colony structure. This makes it more difficult to understand the impact that the network structure might have on transport properties and colony growth.

B. Cellular Automata Models

The first attempts to capture a direct representation of the morphology of the colony were based on cellular automata (CA) operating in discrete time, space and state. Although CA models are discredited, 'growth' is typically controlled through interaction with continuous fields of nutrients or signalling molecules (Ermentrout and Edelstein-Keshet 1993; Liddell and Hansen 1993; Regalado et al. 1996; Lopez and Jensen 2002). CA models can generate crude spatial representations of mycelial structure (Fig. 13.6A), but are heavily constrained by the regular, often two-dimensional lattice used in the simulation. One more recent approach to unite the aspirations of the different types of modelling is to make a hybrid model that captures the most pertinent biological behaviourr in a PDE model, but allows the PDE model to run on a discrete framework that simulates the discrete behavior of individual hyphae and the network structure of the mycelium. This approach has been pioneered by Davidson and colleagues with impressive results (Boswell et al. 2006).

C. Vector Models

An alternative approach to achieve greater morphological realism is to develop models based upon (empirical) rules that govern the growth rate and branching characteristics of vectors representing the hyphae. The rules may include stochastic sampling of experimentally determined parameter distributions of, for example, tip and branch angles, branching frequency or internode length (Hutchinson et al. 1980; Yang et al. 1992a, b; Lejeune and Baron 1995, 1997, 1998; Lejeune et al. 1995). Rather than prescribe these growth and branching parameters, Meškauskas and colleagues (2004a, b) devel-
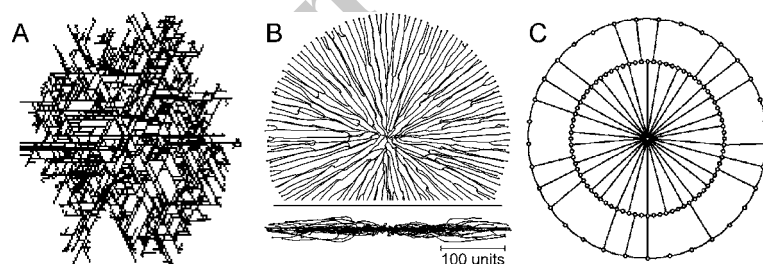

Fig. 13.6. Morphological models of colony growth. **A** The typical output from a cellular automaton model running on a hexagonal grid in which the growth direction and branching probability have a limited degree of stochasticity (M.D. Fricker, unpublished data). **B** Visualizations produced by the neighbour-sensing model of hyphal growth, assuming a negative autotropic reaction and density-dependent branching (branching probability 40% per iteration), with the density field being generated by all of the mycelium.

An additional horizontal plane tropism restricts growth to a thin horizontal zone analogous to a circular colony grown on agar (viewed from above, *upper visualization*) with a narrow profile (side view, *lower visualization*; Meškauskas et al. 2004a). **C** An analytically solvable model showing radial connections from peripheral nodes to an effective hub. The average shortest path can be calculated with varying cost-functions for systems with multiple concentric rings (Jarrett et al. 2006)

oped a Neighbour Sensing (NS) model in which the growth vector of each virtual hyphal tip is calculated taking into account the potential influence of the surrounding virtual mycelium (Fig. 13.6B). Thus in this model branching probability, position and orientation are determined directly by evaluation of local density-dependent fields, rather than through random stochastic processes. The model outputs various colony statistics, such as total mycelial length and internode length, that assist in comparison with real experimental data (Meškauskas et al. 2004a, b).

Other visually realistic simulations have been produced using 'Lindenmayer' (or L) systems. L-Systems are string rewriting rules (productions) operating on a component (predecessor) and converting it to a successor according to the rule(s), so that a complex object can be developed by successive replacement of parts of a simpler object. They were formulated by Lindenmayer (1968) as an axiomatic theory of biological development. L-Systems operate with a string notation which has been given increasing levels of complexity and simulation power over the years (Prusinkiewicz and Lindenmayer 1990; Prusinkiewicz 2004; Prusinkiewicz and Rolland-Lagan 2006; see also the 'visual models of morphogenesis' website at http://www.cpsc.ucalgary.ca/Research/bmv/vmm-deluxe/index.html).

Although branching fungal mycelia fit well with the L-system framework, there has been little application of L-systems to modelling fungi (Liddell and Hansen 1993; Soddell et al. 1995; Tunbridge and Jones 1995). The most sophisticated stochastic context-sensitive parametric L-system so far developed (Tunbridge and Jones 1995) implements the underlying cellular processes originally put forward by Prosser and Trinci (1979). Thus tip growth is dependent on vesicle supply from sub-apical compartments. Once sufficient growth occurs, nuclear division and septum formation take place. If sufficient vesicles subsequently accumulate in subapical segments, branch formation is initiated. Iteration of these rules generates a string describing the branching structure, but with no explicit two- or three-dimensional representation. To produce realistic two-dimensional images, additional stochastic operations are included during visualisation of the structure, such as random selection of branching direction, variation in branching angle, curved hyphal shape and preferential radial growth. The authors note that more realistic graphical depiction would require the introduction of geometrical information into the simulation so that the stochastic elements form part of the developmental rules rather than just affecting visualisation of the structure.

These models all produce branching trees, where the emphasis is to achieve a representative simulation of the structure formed or to investigate plausible mechanisms based on the underlying physiological processes that may control growth. However, none of the vector models include anastomoses, not least because hyphal contact is difficult to calculate in three-dimensional space and cycles are difficult to capture within the hierarchical data structure of either the NS-model or L-model. Thus, none of the current morphological models help to provide any insight into the importance of the network structure. Furthermore, it is not possible to perform much quantitative comparison between the extracted network representations described here and the model simulations in the absence of anastomoses.

D. Abstracted Networks – Hub and Spoke Models

An alternative approach to understand the behaviour of fungal networks is to abstract the essence of a mycelial network and re-cast it in a form that permits more rigorous mathematical analysis. Thus the interplay between radial expansion and lateral connections can be captured in a 'hub and spoke' model of the developing fungal mycelium (Ashton et al. 2005; Jarrett et al. 2006; see Fig. 13.6C). This is a generalised topology applicable to several different (non-biological) transport systems and allows exactly solvable solutions to questions of nutrient flows under different cost scenarios (Ashton et al. 2005; Jarrett et al. 2006). The formula for the average shortest path length across the network comprising a central hub with varying connections (spokes) to a ring of nodes can be calculated and exhibits non-trivial behaviour when different cost functions are imposed on transport through the hub, for example. It is possible to extend this model further to consider a more complicated model of a biological system which contain a ring and hub embedded within another ring, with the original ring–hub motif functioning now as a hub. This process may then be repeated to whatever extent is required by 're-normalising' each ring–hub combination as a hub for the next outer ring, with a cost for using this hub equivalent

to the average shortest path of the original ring–hub motif (Jarrett et al. 2006). This enables analysis of increasingly complex networks by collapsing multiple rings around a very central hub into one structure albeit with a complicated cost function.

IV. Nutrient Transport Through the Network

Although the network architecture is of considerable interest, it only defines which connections are possible at any given time, but not the strength or direction of nutrient transport or signalling fluxes flowing on the network. The precise mechanisms underlying nutrient translocation in fungi are not yet characterised in detail, but are thought to include mass flow, diffusion, generalised cytoplasmic streaming and specific vesicular transport (Jennings 1987; Olsson and Jennings 1991; Olsson and Gray 1998; Cairney 2005; Darrah et al. 2006; see also the chapter by Ashford and Allaway, Chap. 2 in this volume).

A. Transport at the Micron to Millimetre Scale

At the cellular level, many organelles are known to move by motor-driven transport predominantly along the microtubule cytoskeleton, primarily to keep pace with the extending hyphal tip in the apical septal compartment (Fischer 1999; Steinberg 2000; Suelmann and Fischer 2000; Westermann and Prokisch 2002; Hickey et al. 2005; see also the chapters by Fischer and by Sudbery and Court, respectively Chaps. 5 and 6 in this volume). Occasionally much more rapid movements can be observed and may be driven by association with different classes of motor protein (Suelmann and Fischer 2000). For example, during normal growth, migration of the most apical nuclei follows tip elongation, at speeds of $0.1–1.2$ µm min^{-1}, with progressive slowing and eventually arrest sub-apically (Suelmann et al. 1997; Fischer 1999). However, during formation of a dikaryon, nuclear migration can be orders of magnitude higher (Suelmann and Fischer 2000) and nuclei can spread over long distances throughout the whole mycelium of the compatible partner. Whilst the nucleus is not normally considered in discussion of nutrient movement, it has been suggested that mobilisation of N and P from DNA can act as a valuable source of nutrients from an osmotically inactive precursor that can be ex-

ploited under resource limitation or during secondary branch formation in more mature hyphae (Maheshwari 2005).

Movement of material in vesicles along a cytoskeletal system is perhaps a more traditional mechanism to translocate nutrients over long distances. However, at this stage there is little quantitative information documenting the role of vesicle movement in sub-apical compartments, as most research has focussed on vesicle trafficking events at the tip, particularly the evidence for (or against) endocytosis (e.g. Cole et al. 1997; Hoffmann and Mendgen 1998; Fischer-Parton et al. 2000; Atkinson et al. 2002; Torralba and Heath 2002; Read and Kalkman 2003; Steinberg and Fuchs 2004; Harris and Kwang 2006; see also the chapter by Bourett et al., Chap. 1 in this volume). Motor-driven transport along microtubules can operate at speeds of $1–3$ µm s^{-1} (Steinberg 1998, 2000), which is more than sufficient velocity to bring material to an elongating tip, although the flux depends on the volume of the vesicles and the concentration of the nutrients. To be an effective transport system over several septal compartments or even over a whole colony, a microtubule-based system would require persistent polarised arrays extending over a considerable physical distance. Although there is increasing evidence of a role for microtubules in organelle movement (Xiang and Plamann 2003), only a few studies have documented microtubule arrays over the physical scales needed to explain nutrient transport throughout a colony (see, for example Timonen et al. 2001). Likewise, actin microfilaments are essential for polarised growth and septation, and are involved in organelle movement in apical cells (Steinberg 1998, 2000; Czymmek et al. 2005; Harris and Kwang 2006; see also the chapter by Sudbery and Court, Chap. 6 in this volume), but their role has not been studied in the long-distance transport of vesicles on a millimetre scale or higher.

In addition to small vesicle transport, it has been proposed that the highly dynamic pleiomorphic vacuolar system might have a role in long-distance nutrient translocation (Ashford 1998; Ashford and Allaway 2002; Chap. 2 in this volume). This extensive organelle system is present in filamentous fungi of all the major fungal taxonomic groups so far examined (Ashford 1998; Ashford and Allaway 2002). Several mechanisms have been suggested, including diffusion through connected vacuole compartments, directed transport of small vesicles, 'crawling' of large vacuoles and even peristaltic-like contractions (Ashford 1998; Cole

et al. 1998; Bago et al. 2001; Ashford and Allaway 2002; Cairney 2005; see the chapter by Ashford and Allaway, Chap. 2 in this volume). We recently used confocal fluorescence recovery after photobleaching (FRAP) of an internalised fluorescent marker to quantify diffusive transport for different levels of vacuolar organisation moving away from the tip, in combination with a predictive simulation model from these data to determine the transport characteristics of the system over an extended length scale (Darrah et al. 2006). This combined imaging and modelling approach reveals that the vacuole system can have a major impact on solute transport on a millimetre-to-centimetre scale. There is also a strong predicted interaction between vacuolar organisation, available nutrient levels, the predicted diffusion transport distances and the architecture of the branching colony margin. For example, an unbranched hypha possessing a continuous tubular vacuole system can sustain growth over a transport distance ~12–24 mm solely by diffusion through the vacuole system. Conversely, diffusion alone in a maximally branched system would only be sufficient to supply enough resources to the tip over a few millimetres (Darrah et al. 2006).

This poise between translocation being sufficient or insufficient depending on the amount of hyphal branching and status of the vacuolar network suggests that nutrient supply through the vacuolar system could be an important route to co-ordinate tip growth and branching. It is possible that reg-

ulation of the connectivity of the vacuolar system could change its translocation capacity according to the local nutrient demand. The system could thus shift between increasing transport to tips, to preventing unnecessary nutrient mobility by isolating tips. Alternatively, and equally likely, is that the vacuolar system translocates material acquired by the tips back into the main colony, against the mass flow component in the cytoplasm needed for tip extension, particularly when growing over an inert substrate (Fig. 13.7). This problem becomes progressively more acute moving basipetally from the tip, as the acropetal flow through the parent hypha has to increase with the number of tips supported. Some reduction in the flow velocity can be achieved by increasing the diameter of the hypha, particularly as volume flow scales with r^4 (see Eq. 13.1). However, fluorescence labelling of the vacuoles and mitochondria in these regions shows that they are anchored in place and buffeted by a cytoplasmic flow (Ashford 1998; Darrah et al. 2006).

It should be noted that the vacuole model does not preclude additional solute translocation pathways that may operate in parallel in the cytoplasm. We are currently working on the measurement and modelling of cytoplasmic and apoplastic diffusion and mass flow pathways, with a view to building an extended model with all compartments represented. It is expected that this will yield useful predictive results for relatively simple branched mycelial systems in the peripheral growth zone. However, there is still remarkably little understand-
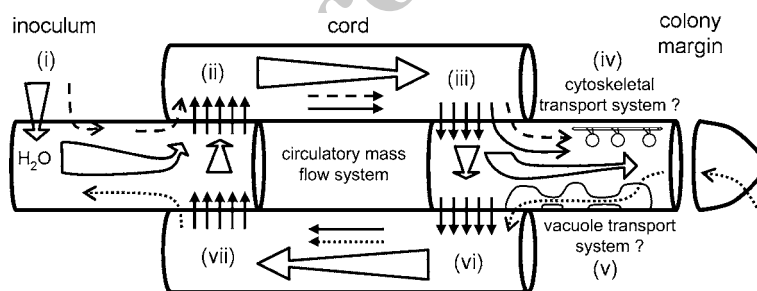

Fig. 13.7. Schematic diagram of possible transport pathways operating in corded mycelial systems. (*i*) Water (*open arrows*) and nutrients (*dashed line*) are initially taken up at the inoculum. (*ii*) An osmotically active solute (*solid arrows*) is loaded into a vessel hypha with a cord to generate an acropetal pressure-driven mass flow that also carries other solutes towards the tips. (*iii*) The osmotic gradient is maintained by solute unloading at the base of the peripheral growth zone. (*iv*) Nutrients needed for growth move towards the tip through a combination of cytoplasmic diffusion, mass flow, vesicle transport and/or diffusion through the vacuole system. Nutrients taken up at the tip have to move backwards against the prevailing direction of mass flow, possibly through the vacuole system (*v*). (*vi*) The majority of the osmotically active solute is loaded into a second vessel hypha to generate a mass flow in the opposite direction to facilitate basipetal transport. (*vii*) Unloading of the solute at the inoculum completes the cycle needed for rapid bi-directional solute movement

ing on how these might interface with the developing sub-marginal anastomosis network and cord formation behind the growth front. Clearly an area for future research is to provide detailed anatomical descriptions of the hyphal organisation in these key areas of the colony, to link cell biological investigations at the hyphal level to flux-based measurements at the colony level.

B. Transport at the Millimetre to Centimetre Scale

Detailed temporal and spatial analysis of nutrient fluxes in individual mycelia uses non-invasive mapping of radioisotopes, mainly ^{14}C and ^{32}P. Typically, the final radiolabel distribution is visualised using autoradiography techniques, phosphor-imaging or analysis by destructive harvesting of the tissues followed by scintillation counting. The emerging picture for C and P dynamics is complex, with evidence from studies in microcosms for highly responsive shifts in nutrient allocation depending upon the size and quality of resource units, the sequence of their encounter and the presence of other competing organisms (Boddy 1999). In general, substantial levels of isotope are taken up, but with varying amounts retained at the loading site (Clipson et al. 1987; Olsson and Gray 1998). Net allocation of the remainder through the network is a complex function of multiple competing source–sink relationships (Wells et al. 1995, 1998, 1999). Movement can be bi-directional (Granlund et al. 1985; Olsson and Gray 1998; Lindahl et al. 2001; Nielsen et al. 2002), with features similar to the operation of a circulatory system (Wells et al. 1998).

Absolute rates of translocation vary over at least two orders of magnitude, from $1.8\,\mathrm{mm\,h^{-1}}$ (Olsson and Gray 1998) to $200\,\mathrm{mm\,h^{-1}}$ (Brownlee and Jennings 1982), depending upon the degree that specific transport pathways, such as cords and rhizomorphs, have developed. The most likely system driving transport over these length scales is mass flow, although how the driving force is established and the precise anatomy, connectivity and control of flux through the conduits are not clear. Unlike a cytoskeletal/motor-driven system, the velocity of movement in a mass flow system is relatively uninformative *per se*, as it is a function of the relative cross-sectional area of the different pipes at each level in the branching hierarchy. For example, the water flow rate through a single cord growing out across an inert surface has to scale linearly with the number of growing tips supported and inversely with the cross-sectional area of conducting tissue in the cord in relation to the cross-sectional area of the individual hyphae. In other branching systems there is typically conservation of cross-sectional area at all levels of the branching hierarchy, giving a constant flow rate (West et al. 1997, 2001). We infer that this is not the case in fungal networks, as the diameter of the cords increases at a lower rate than predicted by an area-preserving relationship and conversely the measured (nutrient) velocities are all significantly greater than the tip extension rate. There is also a major conceptual difficulty in setting up a plausible mass flow model that can accommodate bi-directional movement without extremely tight coupling between inflow and outflow at each end of the system. One solution might be to have specialised cells cycling an osmotically active molecule, such as trehalose, at both ends of two adjacent but insulated conduits to generate anti-parallel mass flow (Fig. 13.7). Other nutrients could be loaded and unloaded at any point of the circulating stream as local source–sink patterns change. Interestingly, the rate of solute movement in the cords in such a circulatory mass flow model could be completely uncoupled from the rate of tip growth.

In comparison to C and P, even less information is available for N dynamics, as there is no suitable radioisotope tracer. However, some progress has been made using ^{14}C-aminoisobutyrate (^{14}C-AIB) as a non-metabolised marker for soluble amino acids (Kim and Roon 1982; Watkinson 1984; Lilly et al. 1990; Olsson and Gray 1998; Tlalka et al. 2002, 2003). ^{14}C-AIB shows rapid uptake, bi-directional transport and movement through specific transport pathways in undifferentiated mycelia on agar (Olsson and Gray 1998). Recently, using photon-counting scintillation imaging (PCSI), we showed that N allocation is extremely dynamic, with rapid, preferential N-resource allocation to C-rich sinks, induction of bi-directional transport on cord formation and abrupt switching between different pre-existing transport routes (Tlalka et al. 2002, 2003). These results suggested that our predictions of transport based solely on the network architecture (see Sect. C.) are too simplistic. However, we believe that the mismatch between predictions from the simple network model and the experimental data will be a productive area for future research and may give much greater insights into the strategy used by the fungus to control fluxes.

Whilst indeterminate growth and flexible resource allocation are of great benefit in exploiting a patchy resource environment (Boddy 1999; Ettema and Wardle 2002; Watkinson et al. 2006), coordination of these activities poses a considerable challenge within an interconnected, but locally responsive, network (Rayner et al. 1994). In this context, it is interesting to note that there is a significant pulsatile component to N-transport, with evidence for differential behaviour between the assimilatory and foraging mycelia. The pulsatile component can be analysed using Fourier techniques to show that signals from the assimilatory hyphae in the inoculum, new resources and the foraging hyphae all oscillate as distinct domains that are locally synchronised, but are out of phase with each other (Fig. 13.3, see page 310; Tlalka et al., submitted). At this stage we do not know what significance to attribute to the emergence of oscillatory phase domains in terms of global co-ordination within the colony. However, there is an extensive literature on the emergent properties of coupled oscillatory systems (see, for example Strogatz 2001) and it is tempting to speculate that coupled oscillatory behaviour may reflect underlying pattern formation in basidiomycete fungi, as with other simple microbial systems (Gerisch 1987; Dormann et al. 2002; Ueda 2005). This may represent a general principle used by self-organising biological systems to achieve global co-ordination and solve complex routing problems (Nakagaki et al. 2000, 2004; Tero et al. 2006).

V. Conclusion: Future Prospects

The past few years have seen massive advances in the technology available to address fundamental questions in fungal biology. Live cell imaging, molecular techniques and green fluorescent protein fusions are set to revolutionise our understanding of sub-cellular dynamics in a similar manner to results in the plant field (Brandizzi et al. 2002; Fricker et al. 2006; see also the chapters by Ashford and Allaway, and Bourett et al., respectively Chaps. 1 and 2 in this volume). New radioisotope imaging techniques are adding dynamics to our understanding of nutrient fluxes at the colony level (Gray et al. 1995; Timonen et al. 1996; Olsson and Gray 1998; Lindahl et al. 2001; Tlalka et al. 2002, 2003), whilst tools from graph theory may start to provide insights into the crucial network organi-

sation and behaviour within the colony. Indeed, it is not impossible that detailed characterisation of such self-organised, adaptive networks and their dynamical behaviour may inform strategies to improve the design of anthropogenic infrastructure networks. Finally, a range of mathematical models is being developed that have the potential to draw together results from all these disparate strands and synthesise a coherent picture of colony growth and function for the first time.

References

Albert R, Barabasi AL (2002) Statistical mechanics of complex networks. Rev Mod Phys 74:47–97

Alon N, Yuster R, Zwick U (1997) Finding and counting given length cycles. Algorithmica 17:209–223

Amaral LAN, Ottino JM (2004) Complex networks – augmenting the framework for the study of complex systems. Eur Phys J B 38:147–162

Ashford AE (1998) Dynamic pleiomorphic vacuole systems: are they endosomes and transport compartments in fungal hyphae? Adv Bot Res 28:119–159

Ashford AE, Allaway WG (2002) The role of the motile tubular vacuole system in mycorrhizal fungi. Plant Soil 244:177–187

Ashton DJ, Jarrett TC, Johnson NF (2005) Effect of congestion costs on shortest paths through complex networks. Phys Rev Lett 94:1–4

Atkinson HA, Daniels A, Read ND (2002) Live-cell imaging of endocytosis during conidial germination in the rice blast fungus, *Magnaporthe grisea*. Fungal Genet Biol 37:233–244

Bago B, Pfeffer P, Shachar-Hill Y (2001) Could the urea cycle be translocating nitrogen in the arbuscular mycorrhizal symbiosis? New Phytol 149:4–8

Ball MO, Provan JS (1983) Calculating bounds on reachability and connectedness in stochastic networks. Networks 13:253–278

Barabasi AL, Albert R (1999) Emergence of scaling in random networks. Science 286:509–512

Barrat A, Barthelemy M, Pastor-Satorras R, Vespignani A (2004) The architecture of complex weighted networks. Proc Natl Acad Sci USA 101:3747–3752

Barrat A, Barthelemy M, Vespignani A (2005) The effects of spatial constraints on the evolution of weighted complex networks. J Stat Mech 5:49–68

Barthelemy M, Barrat A, Pastor-Satorras R, Vespignani A (2005) Characterization and modeling of weighted networks. Physica A 346:34–43

Bartnicki-Garcia S, Hergert F, Gierz G (1989) Computer-simulation of fungal morphogenesis and the mathematical basis for hyphal (tip) growth. Protoplasma 153:46–57

Bezzi M, Ciliberto A (2004) Mathematical modelling of filamentous microorganisms. http://arxivorg/abs/q-bio/0402004

Boddy L (1993) Saprotrophic cord-forming fungi – warfare strategies and other ecological aspects. Mycol Res 97:641–655

Boddy L (1999) Saprotrophic cord-forming fungi: meeting the challenge of heterogeneous environments. Mycologia 91:13–32

Boddy L, Donnelly DP (2006) Fractal geometry and microorganisms in the environment. In: Senesi N, Wilkinson K (eds) Fractal structures and processes in the environment. IUPAC, London

Boddy L, Wells JM, Culshaw C, Donnelly DP (1999) Fractal analysis in studies of mycelium in soil. Geoderma 88:301–328

Boswell GP, Jacobs H, Davidson FA, Gadd GM, Ritz K (2002) Functional consequences of nutrient translocation in mycelial fungi. J Theor Biol 217:459–477

Boswell GP, Jacobs H, Davidson FA, Gadd GM, Ritz K (2003a) Growth and function of fungal mycelia in heterogeneous environments. Bull Math Biol 65:447–477

Boswell GP, Jacobs H, Davidson FA, Gadd GM, Ritz K (2003b) A positive numerical scheme for a mixed-type partial differential equation model for fungal growth. Appl Math Comp 138:321–340

Boswell GP, Jacobs H, Ritz K, Gadd GM, Davidson FA (2006) The development of fungal networks in complex environments. Bull Math Biol. DOI 10.1007/s11538-005-9056-6

Brandizzi F, Fricker M, Hawes C (2002) A greener world: the revolution in plant bioimaging. Nature Rev Mol Cell Biol 3:520–530

Brownlee C, Jennings DH (1982) Long-distance translocation in *Serpula lacrimans* – velocity estimates and the continuous monitoring of induced perturbations. Trans Br Mycol Soc 79:143–148

Buhl J, Gautrais J, Sole RV, Kuntz P, Valverde S, Deneubourg JL, Theraulaz G (2004) Efficiency and robustness in ant networks of galleries. Eur Phys J B 42:123–129

Buller AHR (1931) Researches on fungi, vol 4. Longmans Green, London

Buller AHR (1933) Researches on fungi, vol 5. Longmans Green, London

Cairney JWG (2005) Basidiomycete mycelia in forest soils: dimensions, dynamics and roles in nutrient distribution. Mycol Res 109:7–20

Caldarelli G, Pastor-Satorras R, Vespignani A (2004) Structure of cycles and local ordering in complex networks. Eur Phys J B 38:183–186

Cardillo A, Scellato S, Latora V, Porta S (2006) Structural properties of planar graphs of urban street patterns. Phys Rev E 73:066107

Clipson NJW, Cairney JWG, Jennings DH (1987) The physiology of basidiomycete linear organs.1. Phosphate-uptake by cords and mycelium in the laboratory and the field. New Phytol 105:449–457

Cole L, Hyde GJ, Ashford AE (1997) Uptake and compartmentalisation of fluorescent probes by *Pisolithus tinctorius* hyphae: evidence for an anion transport mechanism at the tonoplast but not for fluid-phase endocytosis. Protoplasma 199:18–29

Cole L, Orlovich DA, Ashford AE (1998) Structure, function, and, motility of vacuoles in filamentous fungi. Fungal Genet Biol 24:86–100

Crawford JW, Ritz K, Young IM (1993) Quantification of fungal morphology, gaseous transport and microbial dynamics in soil – an integrated framework utilizing fractal geometry. Geoderma 56:157–172

Crawford JW, Pachepsky YA, Rawls WJ (1999) Integrating processes in soils using fractal models. Geoderma 88:103–107

Czymmek KJ, Bourett TM, Shao Y, DeZwaan TM, Sweigard JA, Howard RJ (2005) Live-cell imaging of tubulin in the filamentous fungus *Magnaporthe grisea* treated with anti-microtubule and anti-microfilament agents. Protoplasma 225:23–32

Darrah PR, Tlalka M, Ashford A, Watkinson SC, Fricker MD (2006) The vacuole system is a significant intracellular pathway for longitudinal solute transport in basidiomycete fungi. Eukaryot Cell 5:1111–1125

Davidson FA (1998) Modelling the qualitative response of fungal mycelia to heterogeneous environments. J Theor Biol 195:281–292

Davidson FA, Olsson S (2000) Translocation induced outgrowth of fungi in nutrient-free environments. J Theor Biol 205:73–84

Davidson FA, Park AW (1998) A mathematical model for fungal development in heterogeneous environments. Appl Math Lett 11:51–56

Davidson FA, Sleeman BD, Rayner ADM, Crawford JW, Ritz K (1996) Context-dependent macroscopic patterns in growing and interacting mycelial networks. Proc R Soc Lond Ser B 263:873–880

Davidson FA, Sleeman BD, Rayner ADM, Crawford JW, Ritz K (1997) Travelling waves and pattern formation in a model for fungal development. J Math Biol 35:589–608

Donnelly DP, Wilkins MF, Boddy L (1995) An integrated image-analysis approach for determining biomass, radial extent and box-count fractal dimension of macroscopic mycelial systems. Binary 7:19–28

Dormann D, Vasiev B, Weijer CJ (2002) Becoming multicellular by aggregation; The morphogenesis of the social amoebae *Dicyostelium discoideum*. J Biol Phys 28:765–780

Dorogovtsev SN, Mendes JFF (2002) Evolution of networks. Adv Phys 51:1079–1187

Edelstein L (1982) The propagation of fungal colonies – a model for tissue-growth. J Theor Biol 98:679–701

Edelstein L, Segel LA (1983) Growth and metabolism in mycelial fungi. J Theor Biol 104:187–210

Edelstein L, Hadar Y, Chet I, Henis Y, Segel LA (1983) A model for fungal colony growth applied to *Sclerotium rolfsii*. J Gen Microbiol 129:1873–1881

Edelstein-Keshet L, Ermentrout B (1989) Models for branching networks in 2 dimensions. SIAM J Appl Math 49:1136–1157

Ermentrout GB, Edelstein-Keshet L (1993) Cellular automata approaches to biological modeling. J Theor Biol 160:97–133

Ettema CH, Wardle DA (2002) Spatial soil ecology. Trends Ecol Evol 17:177–183

Fischer R (1999) Nuclear movement in filamentous fungi. FEMS Microbiol Rev 23:39–68

Fischer-Parton S, Parton RM, Hickey PC, Dijksterhuis J, Atkinson HA, Read ND (2000) Confocal microscopy of FM4-64 as a tool for analysing endocytosis and vesicle trafficking in living fungal hyphae. J Microsc 198:246–259

Fleissner A, Sarkar S, Jacobson DJ, Roca MG, Read ND, Glass NL (2005) The so locus is required for vegetative cell fusion and postfertilization events in Neurospora crassa. Eukaryot Cell 4:920–930

Freeman LC (1977) Set of measures of centrality based on betweenness. Sociometry 40:35–41

Fricker M, Runions J, Moore I (2006) Quantitative fluorescence microscopy: from art to science. Annu Rev Plant Biol 57:79–107

Geitmann A (2006) Plant and fungal cytomechanics: quantifying and modeling cellular architecture. Can J Bot 84:581–593

Gerisch G (1987) Cyclic-AMP and other signals controlling cell-development and differentiation in Dictyostelium. Annu Rev Biochem 56:853–879

Gierz G, Bartnicki-Garcia S (2001) A three-dimensional model of fungal morphogenesis based on the vesicle supply center concept. J Theor Biol 208:151–164

Glass NL, Jacobson DJ, Shiu PKT (2000) The genetics of hyphal fusion and vegetative incompatibility in filamentous ascomycete fungi. Annu Rev Genet 34:165–186

Glass NL, Rasmussen C, Roca MG, Read ND (2004) Hyphal homing, fusion and mycelial interconnectedness. Trends Microbiol 12:135–141

Gol'dshtein V, Koganov GA, Surdutovich GI (2004) Vulnerability and hierarchy of complex networks. http://arXivorg/abs/cond-mat/0409298

Granlund HI, Jennings DH, Thompson W (1985) Translocation of solutes along rhizomorphs of Armillaria mellea. Trans Br Mycol Soc 84:111–119

Gray SN, Dighton J, Olsson S, Jennings DH (1995) Real-time measurement of uptake and translocation of Cs-137 within mycelium of Schizophyllum commune Fr by autoradiography followed by quantitative image-analysis. New Phytol 129:449–465

Gregory PH (1984) The fungal mycelium: an historical perspective. Trans Br Mycol Soc 82:1–11

Haggett P, Chorley RJ (1969) Network analysis in geography. Arnold, London

Hankin RKS (2006) The resistor array package. http://wwwcranr-projectorg

Harold S, Tordoff GM, Jones TH, Boddy L (2005) Mycelial responses of Hypholoma fasciculare to collembola grazing: effect of inoculum age, nutrient status and resource quality. Mycol Res 109:927–935

Harris SD, Kwang WJ (2006) Cell polarity in filamentous fungi: shaping the mold. Int Rev Cytol 251:41–77

Hickey PC, Jacobson DJ, Read ND, Glass NL (2002) Live-cell imaging of vegetative hyphal fusion in Neurospora crassa. Fungal Genet Biol 37:109–119

Hickey PC, Swift SR, Roca MG, Read ND (2005) Live-cell imaging of filamentous fungi using vital fluorescent dyes and confocal microscopy. Methods Microbiol 34:63–87

Hoffmann J, Mendgen K (1998) Endocytosis and membrane turnover in the germ tube of Uromyces fabae. Fungal Genet Biol 24:77–85

Hutchinson SA, Sharma P, Clarke KR, Macdonald I (1980) Control of hyphal orientation in colonies of Mucor hiemalis. Trans Br Mycol Soc 75:177–191

Isaaks EH, Srivastava RM (1989) Applied geostatistics. Oxford University Press, New York

Jacobs H, Boswell GP, Scrimgeour CM, Davidson FA, Gadd GM, Ritz K (2004) Translocation of carbon by Rhizoctonia solani in nutritionally-heterogeneous microcosms. Mycol Res 108:453–462

Jarrett TC, Ashton DJ, Fricker M, Johnson NF (2006) Interplay between function and structure in complex networks. Phys Rev D 74:026116

Jennings DH (1987) Translocation of solutes in fungi. Biol Rev 62:215–243

Kim KW, Roon RJ (1982) Transport and metabolic effects of alpha-aminoisobutyric-acid in Saccharomyces cerevisiae. Biochim Biophys Acta 719:356–362

Latora V, Marchiori M (2001) Efficient behavior of small-world networks. Phys Rev Lett 87:198701

Latora V, Marchiori M (2003) Economic small-world behavior in weighted networks. Eur Phys J B 32: 249–263

Leake JR, Johnson D, Donnelly DP, Muckle GE, Boddy L, Read DJ (2004) Networks of power and influence: the role of mycorrhizal mycelium in controlling plant communities and agroecosystem functioning. Can J Bot 82:1016–1045

Lejeune R, Baron GV (1995) On the use of morphological measurements for the quantification of fungal growth. Biotechnol Tech 9:327–328

Lejeune R, Baron GV (1997) Simulation of growth of a filamentous fungus in 3 dimensions. Biotechnol Bioeng 53:139–150

Lejeune R, Baron GV (1998) Modeling the exponential growth of filamentous fungi during batch cultivation. Biotechnol Bioeng 60:169–179

Lejeune R, Nielsen J, Baron GV (1995) Morphology of Trichoderma reesei QM-9414 in submerged cultures. Biotechnol Bioeng 47:609–615

Liddell CM, Hansen D (1993) Visualizing complex biological interactions in the soil ecosystem. J Vis Comp Anim 4:3–12

Lilly WW, Higgins SM, Wallweber GJ (1990) Uptake and translocation of 2-aminoisobutyric acid by Schizophyllum commune. Exp Mycol 14:169–177

Lindahl B, Finlay R, Olsson S (2001) Simultaneous, bidirectional translocation of ^{32}P and ^{33}P between wood blocks connected by mycelial cords of Hypholoma fasciculare. New Phytol 150:189–194

Lindenmayer A (1968) Mathematical models for cellular interaction in development, parts I and II. J Theor Biol 18:280–315

Lopez JM, Jensen HJ (2002) Generic model of morphological changes in growing colonies of fungi. Phys Rev E 65:021903

Maheshwari R (2005) Nuclear behavior in fungal hyphae. FEMS Microbiol Lett 249:7–14

Meškauskas A, Fricker MD, Moore D (2004a) Simulating colonial growth of fungi with the Neighbour-Sensing model of hyphal growth. Mycol Res 108:1241–1256

Meškauskas A, McNulty LJ, Moore D (2004b) Concerted regulation of all hyphal tips generates fungal fruit body structures: experiments with computer visualizations produced by a new mathematical model of hyphal growth. Mycol Res 108:341–353

Mihail JD, Obert M, Bruhn JN, Taylor SJ (1995) Fractal geometry of diffuse mycelia and rhizomorphs of *Armillaria* species. Mycol Res 99:81–88

Nakagaki T, Yamada H, Toth A (2000) Maze-solving by an amoeboid organism. Nature 407:470–470

Nakagaki T, Yamada H, Hara M (2004) Smart network solutions in an amoeboid organism. Biophys Chem 107:1–5

Newman MEJ (2003) The structure and function of complex networks. SIAM Rev 45:167–256

Nielsen JS, Joner EJ, Declerck S, Olsson S, Jakobsen I (2002) Phospho-imaging as a tool for visualization and non-invasive measurement of P transport dynamics in arbuscular mycorrhizas. New Phytol 154:809–819

Olsson S (1999) Nutrient translocation and electrical signalling in mycelia. In: Gow NAR, Robson GD, Gadd GM (eds) The fungal colony. Cambridge University Press, Cambridge, pp 25–48

Olsson S (2001) Colonial growth of fungi. In: Howard RJ, Gow NAR (eds) The Mycota, vol VIII. Biology of the fungal cell. Springer, Berlin Heidelberg New York, pp 125–141

Olsson S, Gray SN (1998) Patterns and dynamics of ^{32}P-phosphate and labelled 2-aminoisobutyric acid (^{14}C-AIB) translocation in intact basidiomycete mycelia. FEMS Microbiol Ecol 26:109–120

Olsson S, Jennings DH (1991) Evidence for diffusion being the mechanism of translocation in the hyphae of 3 molds. Exp Mycol 15:302–309

Pringle A, Taylor JW (2002) The fitness of filamentous fungi. Trends Microbiol 10:474–481

Prosser JI (1995a) Kinetics of filamentous growth and branching. In: Gow NAR, Gadd GM (eds) The growing fungus. Chapman and Hall, London, pp 301–318

Prosser JI (1995b) Mathematical modelling of fungal growth. In: Gow NAR, Gadd GM (eds) The growing fungus. Chapman and Hall, London, pp 319–336

Prosser JI, Trinci APJ (1979) Model for hyphal growth and branching. J Gen Microbiol 111:153–164

Prusinkiewicz P (2004) Modelling plant growth and development. Curr Opin Plant Biol 7:79–83

Prusinkiewicz P, Lindenmayer A (1990) The algorithmic beauty of plants. Springer, Berlin Heidelberg New York

Prusinkiewicz P, Rolland-Lagan AG (2006) Modeling plant morphogenesis. Curr Opin Plant Biol 9:83–88

Rayner ADM (1991) The challenge of the individualistic mycelium. Mycologia 83:48–71

Rayner ADM, Griffith GS, Ainsworth AM (1994) Mycelial interconnectedness. In: Gow NAR, Gadd GM (eds) The growing fungus. Chapman and Hall, London, pp 21–40

Rayner ADM, Watkins ZR, Beeching JR (1999) Self-integration – an emerging concept from the fungal mycelium. In: Gow NAR, Robson GD, Gadd GM (eds) The fungal colony. Cambridge University Press, Cambridge, pp 1–24

Read D (1997) Mycorrhizal fungi – the ties that bind. Nature 388:517–518

Read DJ, Perez-Moreno J (2003) Mycorrhizas and nutrient cycling in ecosystems – a journey towards relevance? New Phytol 157:475–492

Read ND, Kalkman ER (2003) Does endocytosis occurr in fungal hyphae? Fungal Genet Biol 39:199–203

Regalado CM, Crawford JW, Ritz K, Sleeman BD (1996) The origins of spatial heterogeneity in vegetative mycelia: a reaction-diffusion model. Mycol Res 100:1473–1480

Ripley BD (2004) Spatial statistics. Wiley, New York

Ritz K, Crawford J (1990) Quantification of the fractal nature of colonies of *Trichoderma viride*. Mycol Res 94:1138–1141

Ritz K, Millar SM, Crawford JW (1996) Detailed visualisation of hyphal distribution in fungal mycelia growing in heterogeneous nutritional environments. J Microbiol Methods 25:23–28

Roca MG, Davide LC, Mendes-Costa MC, Wheals A (2003) Conidial anastomosis tubes in *Colletotrichum*. Fungal Genet Biol 40:138–145

Roca MG, Davide LC, Davide LMC, Schwan RF, Wheals AE (2004) Conidial anastornosis fusion between *Colletotrichum* species. Mycol Res 108:1320–1326

Roca MG, Arlt J, Jeffree CE, Read ND (2005a) Cell biology of conidial anastomosis tubes in *Neurospora crassa*. Eukaryot Cell 4:911–919

Roca MG, Read ND, Wheals AE (2005b) Conidial anastomosis tubes in filamentous fungi. FEMS Microbiol Lett 249:191–198

Simard SW, Durall DM (2004) Mycorrhizal networks: a review of their extent, function, and importance. Can J Bot 82:1140–1165

Simard SW, Perry DA, Jones MD, Myrold DD, Durall DM, Molina R (1997) Net transfer of carbon between ectomycorrhizal tree species in the field. Nature 388:579–582

Soddell F, Seviour R, Soddell J (1995) Using Lindenmayer systems to investigate how filamentous fungi may produce round colonies. Complexity Int 2

Steinberg G (1998) Organelle transport and molecular motors in fungi. Fungal Genet Biol 24: 161–177

Steinberg G (2000) The cellular roles of molecular motors in fungi. Trends Microbiol 8:162–168

Steinberg G, Fuchs U (2004) The role of microtubules in cellular organization and endocytosis in the plant pathogen *Ustilago maydis*. J Microsc 214:114–123

Strogatz SH (2001) Exploring complex networks. Nature 410:268–276

Suelmann R, Fischer R (2000) Nuclear migration in fungi – different motors at work. Res Microbiol 151:247–254

Suelmann R, Sievers N, Fischer R (1997) Nuclear traffic in fungal hyphae: in vivo study of nuclear migration and positioning in *Aspergillus nidulans*. Mol Microbiol 25:757–769

Tero A, Kobayashi R, Nakagaki T (2006) Physarum solver: a biologically inspired method of road-network navigation. Physica A 363:115–119

Timonen S, Finlay RD, Olsson S, Soderstrom B (1996) Dynamics of phosphorus translocation in intact ectomycorrhizal systems: non-destructive monitoring using a beta-scanner. FEMS Microbiol Ecol 19:171–180

Timonen S, Smith FA, Smith SE (2001) Microtubules of the mycorrhizal fungus *Glomus intraradices* in symbiosis with tomato roots. Can J Bot 79:307–313

Tindemans SH, Kern N, Mulder BM (2006) The diffusive vesicle supply center model for tip growth in fungal hyphae. J Theor Biol 238:937–948

Tlalka M, Watkinson SC, Darrah PR, Fricker MD (2002) Continuous imaging of amino-acid translocation in intact mycelia of *Phanerochaete velutina* reveals rapid, pulsatile fluxes. New Phytol 153:173–184

Tlalka M, Hensman D, Darrah PR, Watkinson SC, Fricker MD (2003) Noncircadian oscillations in amino acid transport have complementary profiles in assimilatory and foraging hyphae of *Phanerochaete velutina*. New Phytol 158:325–335

Torralba S, Heath IB (2002) Analysis of three separate probes suggests the absence of endocytosis in *Neurospora crassa* hyphae. Fungal Genet Biol 37:221–232

Trinci APJ, Wiebe MG, Robson GD (1994) The mycelium as an integrated entity. In: Wessels JGH, Meinhardt F (eds) Growth, differentiation and sexuality. Springer, Berlin Heidelberg New York, pp 175–193

Tunbridge A, Jones H (1995) An L-Systems approach to the modeling of fungal growth. J Vis Comp Anim 6:91–107

Ueda T (2005) An intelligent slime mold: a self-organizing system of cell shape and information. In: Armbruster D, Kaneko K, Mikhailov AS (eds) Networks of interacting machines: production organisation in complex industrial systems and biological cells. World Scientific, Singapore, pp 1–35

Watkinson SC (1984) Inhibition of growth and development of *Serpula lacrimans* by the non-metabolized amino-acid analog alpha-aminoisobutyric-acid. FEMS Microbiol Lett 24:247–250

Watkinson SC, Bebber D, Darrah PR, Fricker MD, Tlalka M, Boddy L (2006) The role of wood decay fungi in the carbon and nitrogen dynamics of the forest floor. In: Gadd GM (ed) Fungi in biogeochemical cycles. Cambridge University Press, Cambridge, pp 151–181

Watts DJ, Strogatz SH (1998) Collective dynamics of 'small-world' networks. Nature 393:440–442

Wells JM, Boddy L, Evans R (1995) Carbon translocation in mycelial cord systems of *Phanerochaete velutina* (Dc, Pers) Parmasto. New Phytol 129:467–476

Wells JM, Harris MJ, Boddy L (1998) Temporary phosphorus partitioning in mycelial systems of the cord-forming basidiomycete *Phanerochaete velutina*. New Phytol 140:283–293

Wells JM, Harris MJ, Boddy L (1999) Dynamics of mycelial growth and phosphorus partitioning in developing mycelial cord systems of *Phanerochaete velutina*: dependence on carbon availability. New Phytol 142:325–334

West GB, Brown JH, Enquist BJ (1997) A general model for the origin of allometric scaling laws in biology. Science 276:122–126

West GB, Brown JH, Enquist BJ (2001) A general model for ontogenetic growth. Nature 413:628–631

Westermann B, Prokisch H (2002) Mitochondrial dynamics in filamentous fungi. Fungal Genet Biol 36:91–97

Xiang X, Plamann M (2003) Cytoskeleton and motor proteins in filamentous fungi. Curr Opin Microbiol 6:628–633

Yang H, King R, Reichl U, Gilles ED (1992a) Mathematical-model for apical growth, septation, and branching of mycelial microorganisms. Biotechnol Bioeng 39:49–58

Yang H, Reichl U, King R, Gilles ED (1992b) Measurement and simulation of the morphological development of filamentous microorganisms. Biotechnol Bioeng 39:44–48